

# Evolution of spin and valence states of $(\text{Pr}_{0.7}\text{Sm}_{0.3})_{0.7}\text{Ca}_{0.3}\text{CoO}_3$ at high temperature and high pressure

J. M. Chen,<sup>1,\*</sup> J. M. Lee,<sup>1</sup> S. C. Haw,<sup>1</sup> S. A. Chen,<sup>1</sup> V. Hardy,<sup>2</sup> F. Guillou,<sup>2</sup> S. W. Chen,<sup>1</sup> C. Y. Kuo,<sup>3</sup> C. W. Pao,<sup>1</sup> J. F. Lee,<sup>1</sup> N. Hiraoka,<sup>1</sup> H. Ishii,<sup>1</sup> K. D. Tsuei,<sup>1</sup> and Z. Hu<sup>3,†</sup>

<sup>1</sup>National Synchrotron Radiation Research Center, Hsinchu 30076, Taiwan, Republic of China

<sup>2</sup>Laboratoire CRISMAT, ENSICAEN, UMR 6508 CNRS, 6 Boulevard du Maréchal Juin, 14050 Caen Cedex, France

<sup>3</sup>Max Planck Institute for Chemical Physics of Solids, Nöthnizer Straße 40, 01187 Dresden, Germany

(Received 31 March 2014; revised manuscript received 19 June 2014; published 8 July 2014)

The changes of physical properties occurring at a first-order-like transition among a wide family of  $(\text{Pr}_{1-y}\text{Ln}_y)_{1-x}\text{Ca}_x\text{CoO}_3$  compounds ( $\text{Ln}$  being a lanthanide) are controversially discussed as a transition of  $\text{Co}^{3+}$  ions from states of low spin (LS) to intermediate spin (IS), or from LS to a mixture of LS and high spin (HS). The debate also includes the nature of the spin state of  $\text{Co}^{4+}$ , as well as the degree of valence shift between  $\text{Pr}^{3+}$  and  $\text{Pr}^{4+}$  which accompanies this transition. In the present paper, we investigated the evolution of spin and valence states of Co ions and the valence state of Pr ions in  $(\text{Pr}_{0.7}\text{Sm}_{0.3})_{0.7}\text{Ca}_{0.3}\text{CoO}_3$ , at high temperature up to 750 K and under pressure up to 36.5 GPa. For this purpose, the data of three spectroscopic techniques were combined: high-resolution Co  $K$ -edge partial-fluorescence-yield x-ray absorption spectra, Pr  $L_{2,3}$ -edge x-ray absorption spectra, and Co  $K\beta$  x-ray emission spectra. The spectral weight transfer of the pre-edge peaks of the Co  $K$ -edge spectra reveals a continuous redistribution of  $3d$  electrons between the  $t_{2g}$  and  $e_g$  levels of Co ions, reflecting a gradual increase of the average Co spin state upon heating. This is further confirmed by Co  $K\beta$  x-ray emission spectra, which show an increase of HS  $\text{Co}^{3+}$  population when increasing temperature from 300 to 750 K. Applying high pressure at 300 K, the Co  $K\beta$  x-ray emission spectra indicate a relatively sharp increase of LS  $\text{Co}^{3+}$  population below 4 GPa. Pr  $L_{2,3}$ -edge x-ray absorption spectra of  $(\text{Pr}_{0.7}\text{Sm}_{0.3})_{0.7}\text{Ca}_{0.3}\text{CoO}_3$  exhibit a valence-state transition from  $\text{Pr}^{3+}$  to  $\text{Pr}^{3.26+}$ , occurring predominantly upon applying pressure in the range  $\sim 4$  to  $\sim 12$  GPa. Owing to the charge balance, increasing pressure in this regime induces complex valence and spin-state transitions within the Co ions. Moreover, at high enough pressure, it is found that the  $\text{Co}^{4+}$  can also undergo a spin-state transition (from IS to LS), in addition to that affecting the  $\text{Co}^{3+}$  (HS to LS).

DOI: [10.1103/PhysRevB.90.035107](https://doi.org/10.1103/PhysRevB.90.035107)

PACS number(s): 71.30.+h, 78.70.Dm, 78.70.En, 75.30.Wx

## I. INTRODUCTION

The cobaltates have attracted considerable attention because of their intriguing magnetic and transport properties, such as superconductivity [1], giant magnetoresistance [2], strong thermopower [3], insulator-metal transition [4,5], charge ordering [6], and spin-blockade behavior [6,7]. These astonishing properties are closely correlated with the spin-state degree of freedom of Co ions, primarily the possibility of  $\text{Co}^{3+}$  ions in  $\text{CoO}_6$  octahedra to be in low spin (LS,  $t_{2g}^6 e_g^0$ ,  $S = 0$ ), high spin (HS,  $t_{2g}^4 e_g^2$ ,  $S = 2$ ), or even intermediate spin (IS,  $t_{2g}^5 e_g^1$ ,  $S = 1$ ) states [8–10]. Although less often addressed,  $\text{Co}^{4+}$  in octahedral environment can also adopt various spin states, e.g., the intermediate spin (IS,  $t_{2g}^4 e_g^1$ ,  $S = 3/2$ ) [8] and low spin (LS,  $t_{2g}^5 e_g^0$ ,  $S = 1/2$ ) states [11]. The physical origin for such a variety of spin states is a subtle balance between the Hund's exchange energy and the crystal-field-splitting energy of Co  $3d$  orbitals. Accordingly, the spin states in Co oxides, and in turn their physical properties, can be modified if the crystal-field interaction is varied by either temperature or external pressure.

An important characteristic of the spin-state transition in perovskite-related cobaltates is that it is generally accompanied by a metal-insulator transition (MIT) [12–15]. The occurrence of temperature-induced spin-state transitions indicates a small difference between the crystal-field-splitting

energy and Hund's coupling energy [7,12,16,17]. In particular,  $(\text{Pr}, \text{Ln})_{1-x}\text{Ca}_x\text{CoO}_3$  cobaltates ( $\text{Ln}$ : lanthanide or rare earth) with perovskite structure attract great interest because of their atypical transport and magnetic properties [12,13,18–23]. Although it is now widely admitted that the ability of Pr to adopt intermediate valence between +3 and +4 is a crucial ingredient, the details of the mechanisms at play in these compounds are still unsolved.

The archetypical example of this family of Pr-based perovskite cobaltates is  $\text{Pr}_{0.5}\text{Ca}_{0.5}\text{CoO}_3$ . In contrast to  $\text{LaCoO}_3$  that only contains  $\text{Co}^{3+}$ ,  $\text{Pr}_{0.5}\text{Ca}_{0.5}\text{CoO}_3$  is a mixed-valence compound with 0.5  $\text{Co}^{3+}$  and 0.5  $\text{Co}^{4+}$  per formula unit (f.u.). At room temperature (RT), it is metallic and has a valence  $\text{Pr}^{3+}$ . As temperature is decreased across  $\sim 90$  K a sudden metal-insulator and volume contraction by  $\sim 2\%$  take place. The transition also involves a valence-state modification of Pr ions from  $\text{Pr}^{3+}$  to mixed  $\text{Pr}^{3+}/\text{Pr}^{4+}$ , which is balanced by an increased  $\text{Co}^{3+}$  content, and is accompanied with a crossover of the  $\text{Co}^{3+}$  spin state towards the nonmagnetic LS state [12,24,25]. Recent experiments demonstrated the formation of metallic domains in the insulating low-temperature phase of  $\text{Pr}_{0.5}\text{Ca}_{0.5}\text{CoO}_3$  induced by ultrarapid photoexcitation on a picosecond time scale, making this material of great potential for ultrarapid optical-switching devices [21].

Similar metal-insulator transitions were reported in  $(\text{Pr}_{1-y}\text{Ln}_y)_{1-x}\text{Ca}_x\text{CoO}_3$  ( $\text{Ln} = \text{Sm}, \text{Eu}, \text{Gd}, \text{Tb}, \text{Y}$ ) perovskites, for varied Ca ( $x = 0.3, 0.4, 0.5$ , etc.) and  $\text{Ln}$  ( $y$  between 0 and 0.5) contents [12,17,19,22,23,26]. One of the most documented materials of this family is

\*jmchen@nsrrc.org.tw

†zhiwei.hu@cpfs.mpg.de

(Pr<sub>0.7</sub>Sm<sub>0.3</sub>)<sub>0.7</sub>Ca<sub>0.3</sub>CoO<sub>3</sub>, in which the coupled valence- and spin-state transitions take place at a critical temperature  $T^* \sim 90$  K [23,27,28]. At  $T \gg T^*$ , praseodymium has a valence state Pr<sup>3+</sup> and cobalt has a mixed-valence state made of 0.7 Co<sup>3+</sup> and 0.3 Co<sup>4+</sup> per f.u. Across  $\sim T^*$ , a valence transition involving Pr<sup>3+</sup> to Pr<sup>4+</sup> balanced by Co<sup>4+</sup>-to-Co<sup>3+</sup> changes was reported. Below  $T^*$ , praseodymium thus exhibits a mixed valence Pr<sup>3+</sup>/Pr<sup>4+</sup>, while Co<sup>3+</sup> is in a LS state. At  $T > T^*$ , however, the spin state of Co<sup>3+</sup> is still fiercely debated. Fujita *et al.* proposed that the spin-state crossover from diamagnetic LS Co<sup>3+</sup> to paramagnetic IS Co<sup>3+</sup> was the origin of the metal-insulator transition [23], but spectroscopic results indicated a mixed LS/HS state above the transition temperature [27]. This controversy actually fits in with a much wider debate about the question to know whether the Co<sup>3+</sup> ions in an octahedral coordination have a mixed HS/LS state or an IS state at high temperature. Such a question is an ongoing issue in LaCoO<sub>3</sub> [9,16,29–35], and it is also present in (Pr<sub>1-y</sub>Ln<sub>y</sub>)<sub>1-x</sub>Ca<sub>x</sub>CoO<sub>3</sub> [12,17,19,22,23,27,36] and in other classes of cobaltates such as RBaCo<sub>2</sub>O<sub>5.5</sub> [7,14] and Sr<sub>1-x</sub>Y<sub>x</sub>CoO<sub>3-x</sub> [37,38].

Our work focused on (Pr<sub>0.7</sub>Sm<sub>0.3</sub>)<sub>0.7</sub>Ca<sub>0.3</sub>CoO<sub>3</sub>, a composition showing a rather high concentration of trivalent cobalt (0.7 per f.u. at RT), which is favorable to investigate the controversial issue of the spin state of Co<sup>3+</sup> above  $T^*$ . Moreover, this material allows us to benefit from complementary results recently obtained by spectroscopic investigations below room temperature (on samples of the same batch). Soft x-ray absorption spectra at the Co  $L_{2,3}$  edge of (Pr<sub>0.7</sub>Sm<sub>0.3</sub>)<sub>0.7</sub>Ca<sub>0.3</sub>CoO<sub>3</sub> indicated that the Co<sup>3+</sup> ions have a mixed HS/LS state, whereas Co<sup>4+</sup> stays in the IS state from RT down to 10 K [27]. In the present work, we focused on the properties at high temperature and high pressure. If the previous interpretation of a mixed Co<sup>3+</sup> HS/LS state and a Co<sup>4+</sup> IS state is correct, one should expect a further increase of HS Co<sup>3+</sup> content and possible appearance of LS Co<sup>4+</sup>, upon heating the sample above RT and upon applying pressure, respectively. It is, however, impracticable to obtain the bulk-sensitive soft x-ray Co  $L_{2,3}$  absorption spectrum upon heating pellet powder samples to a temperature much greater than RT in an ultrahigh-vacuum condition. Hard x-ray Co  $K\beta$  x-ray emission spectroscopy (XES) provides accurate information about the local magnetic moment of Co ions, and hence serves as a sensitive probe of the spin-state transitions of materials upon pressurization and heating [39–42]. Moreover, hard x-ray absorption spectroscopy (XAS) at the Co  $K$  edge, especially in the pre-edge region with high resolution by measuring the partial fluorescence yield, is also a sensitive probe of the spin state [36]. The major advantage of the bulk-sensitive hard x-ray spectrum against the soft x-ray absorption at the Co  $L_{2,3}$  edges is the large probe depth; it provides also a possibility to perform high-pressure experiments, which have effects on the spin and valence states of Co ions and Pr ions. In this work, we hence focused on the evolution of the spin and valence states of Co<sup>3+</sup>, Co<sup>4+</sup>, and Pr<sup>3+</sup> in (Pr<sub>0.7</sub>Sm<sub>0.3</sub>)<sub>0.7</sub>Ca<sub>0.3</sub>CoO<sub>3</sub> with temperature and pressure.

## II. EXPERIMENTS

Polycrystalline samples of (Pr<sub>0.7</sub>Sm<sub>0.3</sub>)<sub>0.7</sub>Ca<sub>0.3</sub>CoO<sub>3</sub> (or Pr<sub>0.49</sub>Sm<sub>0.21</sub>Ca<sub>0.3</sub>CoO<sub>3</sub>) were prepared with a solid-state

reaction with highly pure Pr<sub>6</sub>O<sub>11</sub>, Sm<sub>2</sub>O<sub>3</sub>, CaO, and Co<sub>3</sub>O<sub>4</sub> precursors in stoichiometric proportions. The powders were intimately ground and the mixture was pressed into pellets. The pellets were then sintered at 1200 °C in flowing oxygen gas for 36 h. To ensure satisfactory oxygen stoichiometry, the samples were finally annealed at high-pressure (130 bars) O<sub>2</sub> atmosphere for 48 h at 600 °C. The purity of the material was characterized by powder x-ray diffraction that showed a single phase with orthorhombic symmetry and space group  $Pnma$  [23].

Co  $K$ -edge partial-fluorescence-yield (PFY) x-ray absorption and Co  $K\beta$  x-ray emission spectra were measured at the Taiwan inelastic x-ray scattering beamline BL12XU at SPring-8. The undulator beam was made monochromatic with two Si(111) crystals and focused to  $\sim 30 \times 30 \mu\text{m}^2$  at the sample position with two Kilpatrick-Baez (KB) focusing mirrors. The Co  $K\beta$  x-ray emission was collected at 90° from the incident x rays and analyzed with a spectrometer (Johann type) equipped with a spherically bent Ge(444) crystal (radius 1 m) and a solid-state detector (XFlash 1001 type 1201) arranged on a horizontal plane in a Rowland-circle geometry. The overall energy resolution, evaluated from quasielastic scattering from the sample, had full width  $\sim 0.9$  eV at half maximum (FWHM) about the emitted photon energy, 7650 eV. The Co  $K$ -edge energies were calibrated on measuring a standard Co metal foil with the known inflection point of Co  $K$ -edge absorption at 7709 eV. The intensities of all spectra are normalized to the incident beam intensity monitored just before the sample. A Mao-Bell diamond anvil cell with a Be gasket was used for the high-pressure experiment; silicone oil served as a medium to transmit pressure. The pressure in the cell was measured through the Raman line shift of ruby luminescence. The applied pressure was averaged at multiple points of the ruby luminescence before and after each spectral collection.

X-ray absorption spectra at the Pr  $L_2$  edge were measured at beamline BL07C1, with x-ray energy resolution  $\Delta E/E \sim 2 \times 10^{-4}$ , of the National Synchrotron Radiation Research Center (NSRRC) in Taiwan. The Pr  $L_2$ -edge XAS spectra under pressure were recorded with a perforated diamond anvil cell under a transmission mode with ionization chambers as detectors. For high-temperature measurements, the sample was mounted on a Cu support heated with a foil heater device (Mica Thermo) in a vacuum cell.

## III. RESULTS AND DISCUSSION

Figure 1 shows the evolution of the Co  $K\beta$  XES spectra of (Pr<sub>0.7</sub>Sm<sub>0.3</sub>)<sub>0.7</sub>Ca<sub>0.3</sub>CoO<sub>3</sub> with temperature from 300 to 750 K at ambient pressure (AP). The Co  $K\beta$  emission spectrum displays a main line located at  $\sim 7650$  eV, denoted as the  $K\beta_{1,3}$  line, and a broad satellite line located at  $\sim 7637$  eV, denoted as the  $K\beta'$  line, resulting from the exchange interaction between the  $3p$  core hole and the unfilled  $3d$  shell in the final state of the emission. The  $K\beta'$  satellite intensity is known to be proportional to the local spin magnetic moment of the  $3d$  orbitals of the material. In the present study, it is thus a well suited tool to investigate the Co spin states.

At room temperature, the spin state of Co<sup>3+</sup> in (Pr<sub>0.7</sub>Sm<sub>0.3</sub>)<sub>0.7</sub>Ca<sub>0.3</sub>CoO<sub>3</sub> was proposed to be either an IS

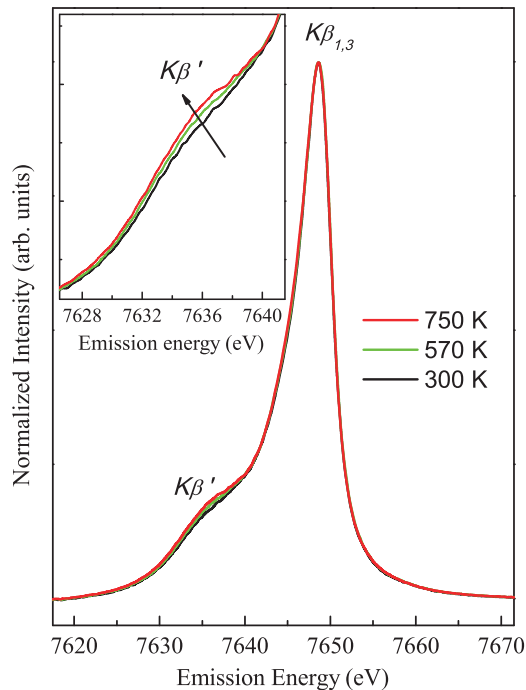


FIG. 1. (Color online) Evolution of the Co  $K\beta$  XES spectra of  $(\text{Pr}_{0.7}\text{Sm}_{0.3})_{0.7}\text{Ca}_{0.3}\text{CoO}_3$  with temperature from RT to 750 K. The inset is an enlargement of the  $K\beta'$  satellite region. An arrow indicates the spectral variations with increasing temperature.

state [23] or a mixed HS/LS state [27]. As shown in the inset of Fig. 1, the  $K\beta'$  satellite intensity increases with increasing temperature above RT, indicating an increasing magnetic moment that can be ascribed to a gradual variation of the spin states of  $\text{Co}^{3+}$ . At this stage, the question remains to know whether this evolution is associated to a transformation from IS to HS or to an increasing HS population in the mixed LS/HS state. To further investigate this gradual spin-state transition at high temperature, Fig. 2 displays high-resolution Co  $K$ -edge XAS spectra of  $(\text{Pr}_{0.7}\text{Sm}_{0.3})_{0.7}\text{Ca}_{0.3}\text{CoO}_3$  in the range 300–750 K. The spectra were obtained in the partial fluorescence yield, with the spectrometer energy fixed at the maximum of the Co  $K\beta_{1,3}$  emission line. The Co  $K$ -edge XAS spectrum of  $(\text{Pr}_{0.7}\text{Sm}_{0.3})_{0.7}\text{Ca}_{0.3}\text{CoO}_3$  in Fig. 2 at RT contains two broad pre-edge lines in the pre-edge region (labeled P1 and P2), an intense white line (labeled B), and two broad lines (labeled C and D) at a greater photon energy.

The main line labeled B in the Co  $K$ -edge XAS spectrum corresponds to an electric-dipole transition of a Co  $1s$  core electron into the Co  $4p$  unoccupied states. The two broad pre-edge lines P1 and P2 are assigned to electric-quadrupole transitions from the Co  $1s$  core level to mainly  $3d t_{2g}$  and  $3d e_g$  levels due to Co  $3d/4p$  hybridization, respectively [36]. In a simplified picture, the lower-energy pre-edge line (P1) and the higher-energy pre-edge line (P2) can be mainly attributed to transition towards the  $t_{2g}$  and  $e_g$  orbitals, respectively [43]. Therefore a close inspection of these lines is particularly relevant to the issue of the  $\text{Co}^{3+}$  spin state. Upon increasing temperature, one observes in the inset of Fig. 2 that P1 gains progressively relative spectral weight and is gradually shifted to smaller energy, whereas P2 loses its spectral weight. This

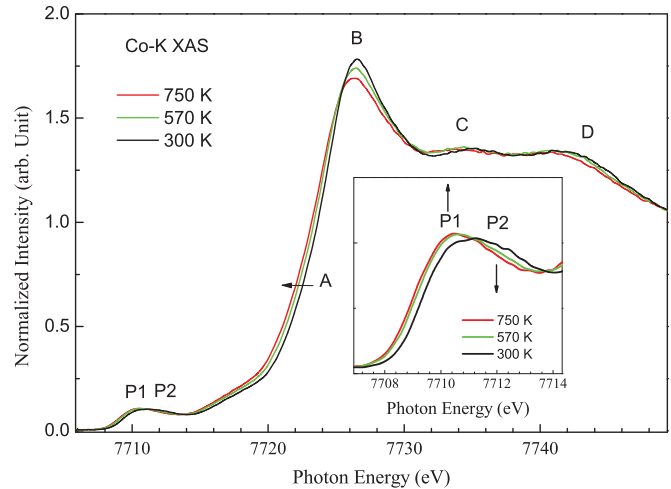


FIG. 2. (Color online) Evolution of the Co  $K$ -edge partial-fluorescence-yield XAS spectra of  $(\text{Pr}_{0.7}\text{Sm}_{0.3})_{0.7}\text{Ca}_{0.3}\text{CoO}_3$  with temperature. The inset shows an enlargement of the pre-edge region. Arrows indicate the spectral variation with increasing temperature. Labels mark the main features discussed in the text.

behavior clearly confirms an increase in the mean spin state of  $\text{Co}^{3+}$  upon heating; Moreover, it suggests that the variation is more pronounced between 300 and 570 K than between 570 and 750 K. Upon increasing temperature, the crystal-field splitting ( $10 Dq$ ) of the Co  $3d$  states decreases. Warming is thus expected to yield a gradual shift of  $\text{Co}^{3+}$  ions from LS towards higher spin states. Such a spectral weight transfer produced by the temperature-induced spin-state transition was reported for  $\text{LaCoO}_3$  [43]. Arrow A in Fig. 2 indicates the absorption edge, defined at a point  $\sim 70\%$  of the normalized data [44,45]. Upon increasing temperature, the increased Co-O distance and HS  $\text{Co}^{3+}$  content lead to a downward shift of the absorption edge of Co  $K$ -edge XAS spectra in Fig. 2, in agreement with previous findings [43].

Applying high pressure generally increases the crystal-field strength by decreasing the Co-O distances, thus increasing the population of LS states among  $\text{Co}^{3+}$  ions; furthermore, pressure also tends to decrease the Pr-O distances, which can favor a higher valence state (on the cubo-octahedral site of the perovskite structure,  $\text{Pr}^{3+}$  and  $\text{Pr}^{4+}$  have cationic radii equal to 1.12 and 0.96 Å, respectively). Actually, the main effect of increasing pressure bears important similarities to that of decreasing temperature. This feature manifests itself in Fig. 3, which shows the pressure dependence of the Pr  $L_2$ -edge XAS spectra of  $(\text{Pr}_{0.7}\text{Sm}_{0.3})_{0.7}\text{Ca}_{0.3}\text{CoO}_3$  at RT. Indeed, one observes that the overall shape of the spectra for 12, 16, and 18.4 GPa at RT is remarkably similar to that recorded at 10 K and ambient pressure (10 K/AP) (red line).

The divalent and trivalent rare-earth elements (e.g.,  $\text{Pr}^{3+}$ ) have a single white line in the  $L_3$  and  $L_2$  edges [46], whereas the tetravalent rare earths (e.g.,  $\text{Pr}^{4+}$ ) exhibit a white line with a double maximum [47–50]. At RT, Pr ions in  $(\text{Pr}_{0.7}\text{Sm}_{0.3})_{0.7}\text{Ca}_{0.3}\text{CoO}_3$  have a valence state purely  $\text{Pr}^{3+}$  and exhibit a single white line at  $\sim 6444.3$  eV (labeled A in Fig. 3) originating from the Pr  $2p \rightarrow 5d$  transitions. The broad spectral feature centered about 14 eV above this line A is assigned to

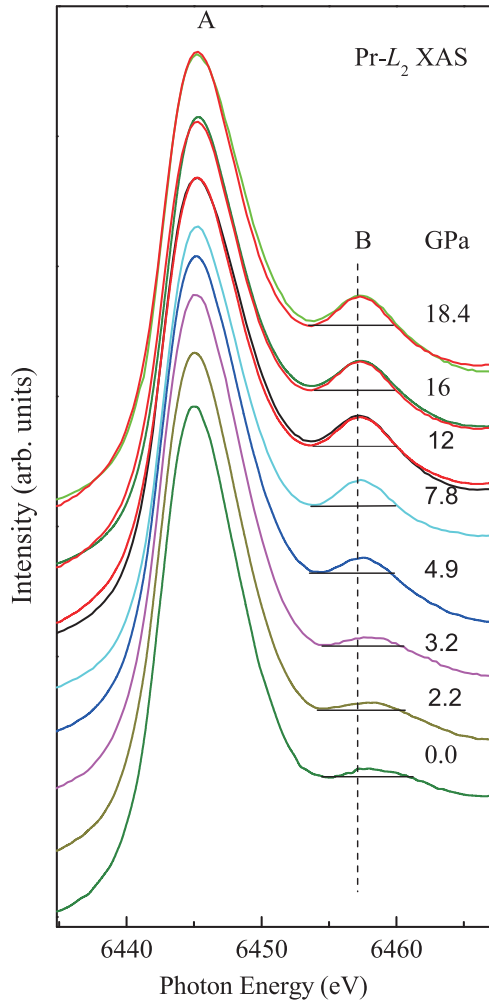


FIG. 3. (Color online) Evolution of the Pr  $L_2$ -edge XAS spectra of  $(\text{Pr}_{0.7}\text{Sm}_{0.3})_{0.7}\text{Ca}_{0.3}\text{CoO}_3$  with pressure at 300 K. The data for 12, 16, and 18.4 GPa at RT are compared with the spectrum (red line) recorded for  $(\text{Pr}_{0.7}\text{Sm}_{0.3})_{0.7}\text{Ca}_{0.3}\text{CoO}_3$  at 10 K/AP.

multiple scattering resonances, as commonly observed in the  $RL_{2,3}$  XAS spectra of  $R_2\text{O}_3$  compounds [51]. We emphasize this feature is too broad to be attributed to a relatively localized  $5d$  state. As pressure is applied, a weak feature labeled B in Fig. 3 (located  $\sim 12$  eV above the main line A) emerges and gradually gains spectral weight. This feature is well known as a higher-energy feature in the double-maximum white line of  $R^{4+}$  compounds, presently ascribable to the dominant final state  $2p^5 4f^1 5d^*$  of  $\text{Pr}^{4+}$  ions [47,48,50]. Note that the lower-energy peak of the white line of  $\text{Pr}^{4+}$  is expected to lie  $\sim 9$  eV below peak B and  $\sim 3$  eV above the main white line peak A [48], which makes it practically undetectable in  $(\text{Pr}_{0.7}\text{Sm}_{0.3})_{0.7}\text{Ca}_{0.3}\text{CoO}_3$  owing to a too small amount of  $\text{Pr}^{4+}$  (see below).

As pressure is increased, the intensity of peak B in the Pr  $L_2$ -edge XAS spectra (see Fig. 3) first increases slightly until 3 GPa, before exhibiting a more pronounced rise within the range  $\sim 4$ –8 GPa, and finally seems to saturate above  $\sim 12$  GPa. The Pr  $L_2$ -edge XAS spectrum of  $(\text{Pr}_{0.7}\text{Sm}_{0.3})_{0.7}\text{Ca}_{0.3}\text{CoO}_3$  at room temperature and ambient pressure (RT/AP) is representative of  $\text{Pr}^{3+}$ , whereas the valence state of Pr ions at

10 K/AP (red line in Fig. 3) is a mixture between  $\text{Pr}^{3+}$  and  $\text{Pr}^{4+}$  with an average valence of  $\text{Pr}^{3.26+}$  [27]. The variation of  $\text{Pr}^{4+}$  content with pressure at RT was quantified as follows: First, the RT/AP spectrum was subtracted from the 10 K/AP spectrum until it had an area of 13% for the “difference spectrum”, i.e., showing the typical features of pure  $\text{Pr}^{4+}$  of  $\text{PrO}_2$ . Following the same procedure as that used in our previous study versus temperature [27], we found that the Pr  $L_2$  spectra above 12 GPa correspond to a mean valence state  $\text{Pr}^{3.26+}$ . This is very close to the value found at 10 K/AP, as it could be anticipated from the very close locations of the spectra in Fig. 3. At pressures below 12 GPa, the fraction of  $\text{Pr}^{4+}$  was derived from the spectral weight in the difference spectrum between a selected pressure spectrum and RT/AP spectrum. The result is shown in Fig. 4. One observes that the  $\text{Pr}^{3+}$  content per f.u. of  $(\text{Pr}_{0.7}\text{Sm}_{0.3})_{0.7}\text{Ca}_{0.3}\text{CoO}_3$  shows a small decrease for pressure below  $\sim 3$  GPa; then it undergoes a notable decrease for pressure ranging between  $\sim 4$  and 8 GPa; finally, it attains  $\sim 0.36 \text{ Pr}^{3+}$  and  $\sim 0.13 \text{ Pr}^{4+}$  per f.u. with an average valence  $\text{Pr}^{3.26+}$  above  $\sim 12$  GPa. We note that such a three-step process is qualitatively similar to that previously observed as a function of temperature between 300 and 10 K [27], as shown in Fig. 4.

Figure 5 shows the evolution of the representative Co  $K\beta$  x-ray emission line of  $(\text{Pr}_{0.7}\text{Sm}_{0.3})_{0.7}\text{Ca}_{0.3}\text{CoO}_3$  as a function of pressure from RT/AP to room temperature and 36.5 GPa (RT/36.5 GPa). As displayed in the inset of Fig. 5, the  $K\beta'$  intensity progressively decreases with increasing pressure, indicating a significant loss of magnetic moment of  $(\text{Pr}_{0.7}\text{Sm}_{0.3})_{0.7}\text{Ca}_{0.3}\text{CoO}_3$ . At pressures above 25 GPa, the  $K\beta'$  satellite line nearly vanishes and the main line  $K\beta_{1,3}$  becomes narrower, leading to an overall spectrum similar to that of  $\text{LaCoO}_3$  at low temperatures [43], indicating that the LS state of Co ions is attained [52]. Accordingly, the results of Fig. 5 strongly suggest that  $(\text{Pr}_{0.7}\text{Sm}_{0.3})_{0.7}\text{Ca}_{0.3}\text{CoO}_3$  undergoes a

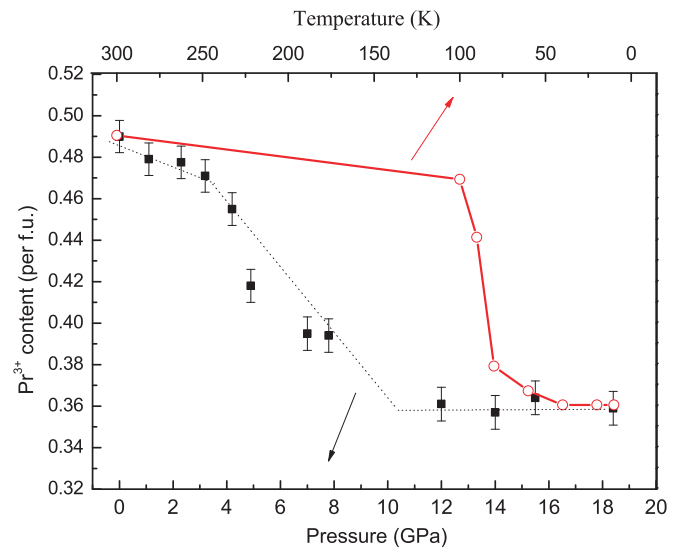


FIG. 4. (Color online) Pressure dependence (solid squares) and temperature dependence (open circles) of the  $\text{Pr}^{3+}$  content per f.u. in  $(\text{Pr}_{0.7}\text{Sm}_{0.3})_{0.7}\text{Ca}_{0.3}\text{CoO}_3$  at RT and AP, respectively. The data of temperature dependence of the  $\text{Pr}^{3+}$  content per f.u. below RT are taken from Ref. [27]. The dashed line is only a guide for the eye.

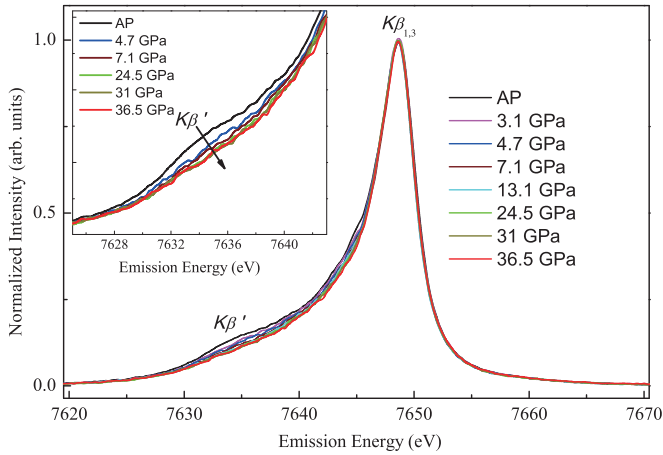


FIG. 5. (Color online) Evolution of the Co  $K\beta$  x-ray emission spectra of  $(\text{Pr}_{0.7}\text{Sm}_{0.3})_{0.7}\text{Ca}_{0.3}\text{CoO}_3$  as a function of pressure from RT/AP to RT/36.5 GPa. The inset is an enlargement of the  $K\beta'$  satellite region. An arrow indicates the spectral variation with increasing pressure.

configuration change of  $\text{Co}^{3+}$  from HS/LS (or IS) to LS states when external pressure is applied at RT [23,27,36].

To extract more quantitative information about the spin magnetic moment from the Co  $K\beta$  emission spectra, we calculated the integrated absolute difference ( $IAD = \sum |I_T - I_{HP}|$ ) as a function of temperature and pressure, with respect to RT/36.5 GPa;  $I_T$  and  $I_{HP}$  denote the normalized intensities of emission spectra for the high-temperature and high-pressure phases, respectively. The integrated absolute value of difference spectra is a method widely applied to deduce exactly the spin magnetic moment from the  $K\beta$  emission spectra [41–43]. It was reported that the  $IAD$  values correlate linearly with the change in the average spin of transition-metal ions [41–43]. The procedure applied to the Co  $K\beta$  emission spectra to obtain the  $IAD$  values involves several steps: (i) normalization of the spectral area, (ii) shifting of the spectra to the same center of mass, (iii) subtraction of a reference spectrum (at 36.5 GPa in the present case) from all spectra, and (iv) integration of the absolute values of these difference spectra. In the present study, the  $IAD$  values were derived using the energy range 7612–7680 eV.

Figure 6 shows the  $IAD$  values deduced from the Co  $K\beta$  emission spectra of  $(\text{Pr}_{0.7}\text{Sm}_{0.3})_{0.7}\text{Ca}_{0.3}\text{CoO}_3$  as a function of applied pressure and temperature. In the evolution versus pressure, several regimes can be distinguished, even though there are no sharp boundaries separating them: First,  $IAD$  decreases rapidly upon pressure application until about  $\sim 4$  GPa; second, it slows down within the range 4–12 GPa; third, there is a wide range (12–25 GPa) along which  $IAD$  decreases slowly and almost linearly; finally,  $IAD$  becomes virtually equal to zero for pressure above 25 GPa. We observed a total  $IAD$  change  $\sim 0.11$  in proceeding from high temperature at 750 K and ambient pressure (750 K/AP) to high pressure at RT/36.5 GPa. This value turns out to be slightly less than that corresponding to a complete HS-to-LS transition of  $\text{Co}^{3+}$  ( $\sim 0.15$ ) [52].

In the inset of Fig. 6, we compare two different spectra of the  $K\beta$  emission; one is the difference between RT/AP and RT/36.5 GPa (red circles), the other is the difference

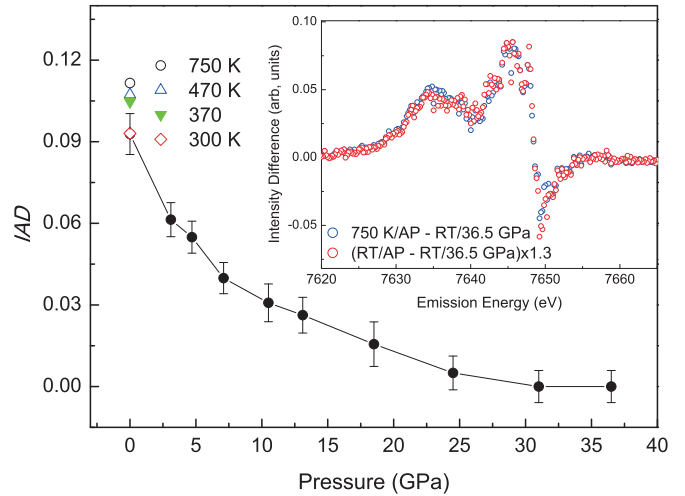


FIG. 6. (Color online)  $IAD$  values of  $(\text{Pr}_{0.7}\text{Sm}_{0.3})_{0.7}\text{Ca}_{0.3}\text{CoO}_3$  as a function of applied pressure and temperature. The inset shows the difference spectrum of the Co  $K\beta$  emission line between RT/AP and RT/36.5 GPa (red open circles) and the difference spectrum of the emission line between 750 K/AP and RT/36.5 GPa (blue open squares).

between 750 K/AP and RT/36.5 GPa (blue squares). We selected the RT/36.5 GPa spectrum as the reference, since it shows the lowest  $K\beta'$  intensity—i.e., the smallest spin magnetic moment of Co ions—within our set of data on  $(\text{Pr}_{0.7}\text{Sm}_{0.3})_{0.7}\text{Ca}_{0.3}\text{CoO}_3$ . Apart from a multiplicative factor, it is clear that the spectral shape of the red circles is nearly identical to that of the blue circles which corresponds to a large content of HS  $\text{Co}^{3+}$  (750 K). This observation strongly supports the fact that at RT/AP the system is most likely not in an IS state, but rather in a mixed HS/LS state; otherwise, one should observe difference spectra having much more contrasted shapes [43].

The  $IAD$  value was shown to vary linearly with the spin of Co ions [41–43], i.e.,

$$IAD(\text{Co}^{3+}) = \alpha S(\text{Co}^{3+}), \quad (1)$$

with  $\alpha = 0.075$  for  $\text{Co}^{3+}$  known from previous work [52], and

$$IAD(\text{Co}^{4+}) = \beta S(\text{Co}^{4+}), \quad (2)$$

whereas  $\beta$  is unknown as no experimental  $\text{Co}^{4+}$   $K\beta$  XES data are available.

For mixed  $\text{Co}^{3+}/\text{Co}^{4+}$  in  $(\text{Pr}_{0.7}\text{Sm}_{0.3})_{0.7}\text{Ca}_{0.3}\text{CoO}_3$  at the pressure  $P_i$ , one can thus consider

$$IAD_{P_i}(\text{Co}^{3+} + \text{Co}^{4+}) = \alpha S_{P_i}(\text{Co}^{3+}) + \beta S_{P_i}(\text{Co}^{4+}). \quad (3)$$

According to a previous XAS investigation of  $(\text{Pr}_{0.7}\text{Sm}_{0.3})_{0.7}\text{Ca}_{0.3}\text{CoO}_3$  [27], the population of Co ions at RT/AP is composed of  $\sim 38\%$  HS  $\text{Co}^{3+}$ ,  $\sim 32\%$  LS  $\text{Co}^{3+}$ , and  $\sim 30\%$  IS  $\text{Co}^{4+}$ . From Eq. (3) and the experimental  $IAD$  value at RT/AP, we can estimate  $\beta = 0.0795$ .

The total  $IAD$  change under pressure is related to not only the spin-state evolution of Co ions, but also the content of  $\text{Co}^{3+}$ . It turns out that pressure induces in  $(\text{Pr}_{0.7}\text{Sm}_{0.3})_{0.7}\text{Ca}_{0.3}\text{CoO}_3$  a partial valence transition from  $\text{Pr}^{3+}$  to  $\text{Pr}^{4+}$ , accompanied with a corresponding transition from  $\text{Co}^{4+}$  to  $\text{Co}^{3+}$ , as required

by charge balance. Accordingly, the content of  $\text{Co}^{3+}$  in the title compound increases with pressure, following the same functional form as that of the mean Pr valence. Knowing the experimental *IAD* values in Fig. 6 and the evolution of  $\text{Pr}^{3+}/\text{Pr}^{4+}$  content per f.u. with pressure in Fig. 4, we then calculated the fractions of the IS  $\text{Co}^{4+}$ , LS  $\text{Co}^{4+}$ , HS  $\text{Co}^{3+}$ , and LS  $\text{Co}^{3+}$  in  $(\text{Pr}_{0.7}\text{Sm}_{0.3})_{0.7}\text{Ca}_{0.3}\text{CoO}_3$  as a function of pressure; the results appear in Fig. 7(a). Based on the spin population of Co ions in Fig. 7(a) and the evolution of  $\text{Pr}^{3+}/\text{Pr}^{4+}$  content per f.u. with pressure in Fig. 4, we divided the pressure response of the valence and spin states of Co ions into three regimes. The first stage is for pressure ranging from AP to  $\sim 4$  GPa, in which the rapidly decreasing magnetic moment of Co ions mainly originates from a HS to LS spin-state evolution of  $\text{Co}^{3+}$  ions, without notable impact of the Pr valence change since it remains very tiny in this range. By contrast, in the second step from  $\sim 4$  to  $\sim 12$  GPa, there is a significant increase in the  $\text{Pr}^{4+}$  content and thus in the mean Pr valence (reaching  $\text{Pr}^{3.26+}$ ), leading to a more determinant influence of the IS  $\text{Co}^{4+} \rightarrow$  LS  $\text{Co}^{4+}$  crossover, running concurrently with the still present HS  $\text{Co}^{3+} \rightarrow$  LS  $\text{Co}^{3+}$  conversion. In the third step above  $\sim 12$  GPa,

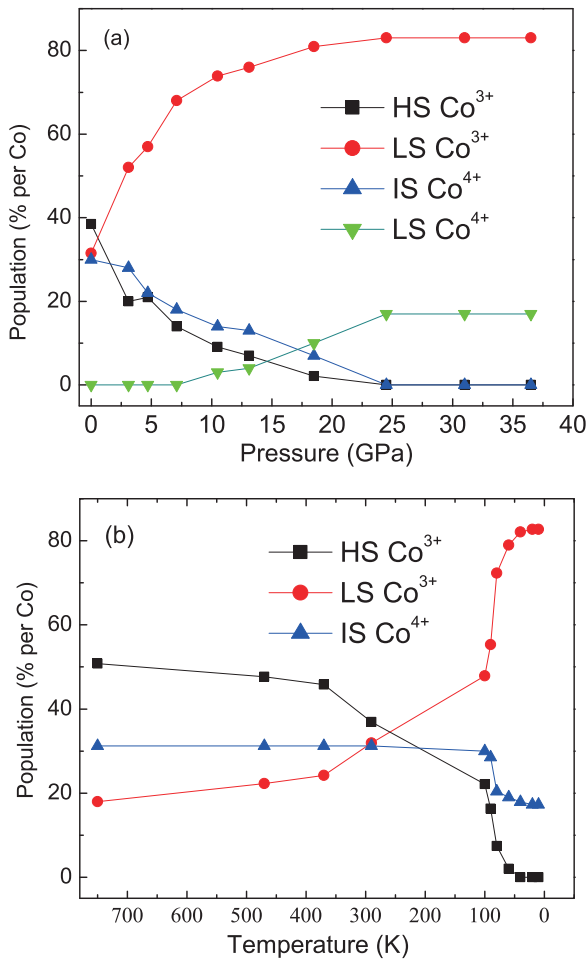


FIG. 7. (Color online) Populations of IS  $\text{Co}^{4+}$ , LS  $\text{Co}^{4+}$ , HS  $\text{Co}^{3+}$ , and LS  $\text{Co}^{3+}$  in  $(\text{Pr}_{0.7}\text{Sm}_{0.3})_{0.7}\text{Ca}_{0.3}\text{CoO}_3$  (a) as a function of pressure from RT/AP to RT/36.5 GPa, and (b) as a function of temperature from 750 K/AP to 10 K/AP (low-temperature data are taken from Ref. [27]).

the valence transition of Pr is completed; thus the  $\text{Co}^{3+}$  and  $\text{Co}^{4+}$  contents remain constant, i.e., 0.83 and 0.17 per f.u., respectively.

When approaching 25 GPa, the  $\text{Co}^{3+}$  content rapidly vanishes and the HS  $\text{Co}^{3+} \rightarrow$  LS  $\text{Co}^{3+}$  transformation cannot account for the whole *IAD* change within the range 12–25 GPa. Actually, one must invoke an increasing influence of a spin-state crossover of the  $\text{Co}^{4+}$  between the IS and LS states. Pressure is indeed expected to favor LS  $\text{Co}^{4+}$  at the expense of IS  $\text{Co}^{4+}$ , still owing to an enhancement of the crystal-field effects as the bond lengths shrink. Even though the  $\text{Co}^{4+}$  content is rather small in our compound, and despite the fact that the change of the spin magnetic moment of  $\text{Co}^{4+}$  ions (from  $3/2$  to  $1/2$ ) is less than that of  $\text{Co}^{3+}$  ions (from 2 to 0), this IS  $\text{Co}^{4+} \rightarrow$  LS  $\text{Co}^{4+}$  transformation leads to a slight reduction of *IAD* values. Above 25 GPa, no more *IAD* change is detected and one can consider that all  $\text{Co}^{3+}$  and  $\text{Co}^{4+}$  are shifted to LS states.

The total *IAD* change,  $\sim 0.11$ , of Co ions from RT/35 GPa to 750 K/AP is smaller than that of a complete LS-to-HS transition of all  $\text{Co}^{3+}$  ions. As shown in Fig. 7(b) about a quarter of  $\text{Co}^{3+}$  ions in  $(\text{Pr}_{0.7}\text{Sm}_{0.3})_{0.7}\text{Ca}_{0.3}\text{CoO}_3$  are still in the LS state at 750 K. Because HS  $\text{Co}^{3+}$  has a larger ionic radius than LS  $\text{Co}^{3+}$ , an increased HS  $\text{Co}^{3+}$  population upon heating leads to an increased local crystal field (i.e., increased  $10 Dq$ ) acting on the remaining LS  $\text{Co}^{3+}$  ions, and consequently hinders a complete transition LS to HS. Accordingly, even at temperatures as high as 750 K (at AP), not all the  $\text{Co}^{3+}$  ions are in the HS state.

#### IV. CONCLUSION

We probed the spin state and valence state of  $\text{Co}^{3+}$ ,  $\text{Co}^{4+}$ , and  $\text{Pr}^{3+}$  in  $(\text{Pr}_{0.7}\text{Sm}_{0.3})_{0.7}\text{Ca}_{0.3}\text{CoO}_3$ , at high temperature and high pressure, with Co *K*-edge partial-fluorescence-yield x-ray absorption spectra, the Pr *L*<sub>2</sub>-edge x-ray absorption spectra, and the Co *K* $\beta$  x-ray emission spectra. Upon increasing temperature from RT up to 750 K, the lower-energy pre-edge line of the Co *K*-edge absorption spectra progressively gained spectral weight, at the expense of the higher-energy pre-edge line. This spectral weight transfer reveals a continuous redistribution of *3d* electrons between the *t*<sub>2g</sub> and *e*<sub>g</sub> levels of  $\text{Co}^{3+}$  ions, as expected for a gradual crossover from LS to higher spin states. Within the whole investigated range (RT–750 K), our observations qualitatively support the achievement of a mixture between LS and HS states of  $\text{Co}^{3+}$  ions. Furthermore, the intensity of the *K* $\beta'$  satellite of Co *K* $\beta$  x-ray emission gradually increases as temperature is increased from RT to 750 K, which corresponds to a gain of magnetic moment well consistent with an increased population of the high-spin state of  $\text{Co}^{3+}$  in  $(\text{Pr}_{0.7}\text{Sm}_{0.3})_{0.7}\text{Ca}_{0.3}\text{CoO}_3$  upon heating.

The intensity of the *K* $\beta'$  satellite in the Co *K* $\beta$  x-ray emission rapidly decreases with increasing pressure below 4 GPa, indicating a notable HS-to-LS spin-state evolution among the  $\text{Co}^{3+}$  ions. Concurrently, the Pr *L*<sub>2</sub>-edge x-ray absorption spectra exhibit a pressure-induced valence transition of Pr ions from  $\text{Pr}^{3+}$  to  $\text{Pr}^{3.26+}$ , taking place predominantly in the range  $\sim 4$ –12 GPa, in a way strikingly similar to what happens as the temperature is lowered across  $\sim 90$  K at AP [27]. A gradually

decreasing intensity of the  $K\beta'$  satellite line in this pressure range is assigned to both increasing (decreasing) content of  $\text{Co}^{3+}$  ( $\text{Co}^{4+}$ ) ions—as required by charge balance—and the continuing HS-to-LS transition of  $\text{Co}^{3+}$  ions. Above 12 GPa, the valence state of Pr ion ( $\text{Pr}^{3.26+}$ ) is scarcely altered; the valence state of Co ions thus remains nearly constant. The observed decreasing intensity of the  $K\beta'$  satellite line might involve a spin-state evolution of  $\text{Co}^{4+}$  ions from an IS ( $S = 3/2$ ) to a LS ( $S = 1/2$ ) state until  $\sim 25$  GPa. At pressures above 25 GPa, the  $K\beta'$  satellite peak nearly vanished and the

main line  $K\beta_{1,3}$  narrowed, corresponding to a LS state for both  $\text{Co}^{3+}$  and  $\text{Co}^{4+}$  in  $(\text{Pr}_{0.7}\text{Sm}_{0.3})_{0.7}\text{Ca}_{0.3}\text{CoO}_3$ .

#### ACKNOWLEDGMENTS

We thank the NSRRC staff for their technical support and L. H. Tjeng for valuable discussions. NSRRC and National Science Council of the Republic of China (Grant No. NSC 102-2113-M-213-004) supported this work.

- 
- [1] K. Takada, H. Sakurai, E. Takayama-Muromachi, F. Izumi, R. A. Dilanian, and T. Sasaki, *Nature (London)* **422**, 53 (2003).
- [2] J. Perez, J. Garcia, J. Blasco, and J. Stankiewicz, *Phys. Rev. Lett.* **80**, 2401 (1998).
- [3] I. Terasaki, Y. Sasago, and K. Uchinokura, *Phys. Rev. B* **56**, R12685 (1997).
- [4] R. R. Heikes, R. C. Miller, and R. Mazelsky, *Physica (Amsterdam)* **30**, 1600 (1964).
- [5] P. M. Raccach and J. B. Goodenough, *Phys. Rev.* **155**, 932 (1967).
- [6] C. F. Chang, Z. Hu, Hua Wu, T. Burnus, N. Hollmann, M. Benomar, T. Lorenz, A. Tanaka, H.-J. Lin, H. H. Hsieh, C. T. Chen, and L. H. Tjeng, *Phys. Rev. Lett.* **102**, 116401 (2009).
- [7] A. Maignan, V. Caignaert, B. Raveau, D. Khomskii, and G. Sawatzky, *Phys. Rev. Lett.* **93**, 026401 (2004).
- [8] R. H. Potze, G. A. Sawatzky, and M. Abbate, *Phys. Rev. B* **51**, 11501 (1995).
- [9] M. A. Korotin, S. Yu. Ezhov, I. V. Solovyev, V. I. Anisimov, D. I. Khomskii, and G. A. Sawatzky, *Phys. Rev. B* **54**, 5309 (1996).
- [10] K. Knížek, P. Novák, and Z. Jirák, *Phys. Rev. B* **71**, 054420 (2005).
- [11] H.-J. Lin, Y. Y. Chin, Z. Hu, G. J. Shu, F. C. Chou, H. Ohta, K. Yoshimura, S. Hébert, A. Maignan, A. Tanaka, L. H. Tjeng, and C. T. Chen, *Phys. Rev. B* **81**, 115138 (2010).
- [12] S. Tsubouchi, T. Kyômen, M. Itoh, P. Ganguly, M. Oguni, Y. Shimojo, Y. Morii, and Y. Ishii, *Phys. Rev. B* **66**, 052418 (2002).
- [13] J. L. García-Muñoz, C. Frontera, A. J. Barón-González, S. Valencia, J. Blasco, R. Feyerherm, E. Dudzik, R. Abrudan, and F. Radu, *Phys. Rev. B* **84**, 045104 (2011).
- [14] C. Martin, A. Maignan, D. Pelloquin, N. Nguyen, and B. Raveau, *Appl. Phys. Lett.* **71**, 1421 (1997).
- [15] Y. Moritomo, T. Akimoto, M. Takeo, A. Machida, E. Nishibori, M. Takata, M. Sakata, K. Ohoyama, and A. Nakamura, *Phys. Rev. B* **61**, R13325 (2000).
- [16] M. W. Haverkort, Z. Hu, J. C. Cezar, T. Burnus, H. Hartmann, M. Reuther, C. Zobel, T. Lorenz, A. Tanaka, N. B. Brookes, H. H. Hsieh, H.-J. Lin, C. T. Chen, and L. H. Tjeng, *Phys. Rev. Lett.* **97**, 176405 (2006).
- [17] K. Knížek, J. Hejtmánek, P. Novák, and Z. Jirák, *Phys. Rev. B* **81**, 155113 (2010).
- [18] P. Tong, Y. Wu, B. Kim, D. Kwon, J. M. S. Park, and B. G. Kim, *J. Phys. Soc. Jpn.* **78**, 034702 (2009).
- [19] S. Tsubouchi, T. Kyômen, M. Itoh, and M. Oguni, *Phys. Rev. B* **69**, 144406 (2004).
- [20] J. Hejtmánek, E. Šantavá, K. Knížek, M. Maryško, Z. Jirák, T. Naito, H. Sasaki, and H. Fujishiro, *Phys. Rev. B* **82**, 165107 (2010).
- [21] Y. Okimoto, X. Peng, M. Tamura, T. Morita, K. Onda, T. Ishikawa, S. Koshihara, N. Todoroki, T. Kyomen, and M. Itoh, *Phys. Rev. Lett.* **103**, 027402 (2009).
- [22] T. Fujita, T. Miyashita, Y. Yasui, Y. Kobayashi, M. Sato, E. Nishibori, M. Sakata, Y. Shimojo, N. Igawa, Y. Ishii, K. Kakurai, T. Adachi, Y. Ohishi, and M. Takata, *J. Phys. Soc. Jpn.* **73**, 1987 (2004).
- [23] T. Fujita, S. Kawabata, M. Sato, N. Kurita, M. Hedo, and Y. Uwatoko, *J. Phys. Soc. Jpn.* **74**, 2294 (2005).
- [24] A. J. Barón-González, C. Frontera, J. L. García-Muñoz, J. Blasco, and C. Ritter, *Phys. Rev. B* **81**, 054427 (2010).
- [25] A. Chichev, J. Hejtmánek, Z. Jirák, K. Knížek, M. Maryško, M. Dlouhá, and S. Vratilav, *J. Magn. Magn. Mater.* **316**, e728 (2007).
- [26] J. Hejtmánek, Z. Jirák, O. Kaman, K. Knížek, E. Šantavá, K. Nitta, T. Naito, and H. Fujishiro, *Eur. Phys. J. B* **86**, 305 (2013).
- [27] F. Guillou, Q. Zhang, Z. Hu, C. Y. Kuo, Y. Y. Chin, H. J. Lin, C. T. Chen, A. Tanaka, L. H. Tjeng, and V. Hardy, *Phys. Rev. B* **87**, 115114 (2013).
- [28] V. Hardy, F. Guillou, and Y. Bréard, *J. Phys.: Condens. Matter* **25**, 246003 (2013).
- [29] A. Podlesnyak, S. Streule, J. Mesot, M. Medarde, E. Pomjakushina, K. Conder, A. Tanaka, M. W. Haverkort, and D. I. Khomskii, *Phys. Rev. Lett.* **97**, 247208 (2006).
- [30] C. He, H. Zheng, J. F. Mitchell, M. L. Foo, R. J. Cava, and C. Leighton, *Appl. Phys. Lett.* **94**, 102514 (2009).
- [31] J. Kunes and V. Krapek, *Phys. Rev. Lett.* **106**, 256401 (2011).
- [32] A. Ishikawa, J. Nohara, and S. Sugai, *Phys. Rev. Lett.* **93**, 136401 (2004).
- [33] D. Phelan, D. Louca, S. Rosenkranz, S.-H. Lee, Y. Qiu, P. J. Chupas, R. Osborn, H. Zheng, J. F. Mitchell, J. R. D. Copley, J. L. Sarrao, and Y. Moritomo, *Phys. Rev. Lett.* **96**, 027201 (2006).
- [34] A. Laref, S. Laref, and S. Bin-Omran, *J. Comput. Chem.* **33**, 673 (2012).
- [35] M. M. Altarawneh, G.-W. Chern, N. Harrison, C. D. Batista, A. Uchida, M. Jaime, D. G. Rickel, S. A. Crooker, C. H. Mielke, J. B. Betts, J. F. Mitchell, and M. J. R. Hoch, *Phys. Rev. Lett.* **109**, 037201 (2012).

- [36] J. Herrero-Martín, J. L. García-Muñoz, K. Kvashnina, E. Gallo, G. Subías, J. A. Alonso, and A. J. Barón-González, *Phys. Rev. B* **86**, 125106 (2012).
- [37] Y. Zhang, S. Sasaki, and M. Izumi, *Phys. Status Solidi B* **244**, 4550 (2007).
- [38] W. Kobayashi, S. Yoshida, and I. Terasaki, *J. Phys. Soc. Jpn.* **75**, 103702 (2006).
- [39] J.-P. Rueff, C.-C. Kao, V. V. Struzhkin, J. Badro, J. Shu, R. J. Hemley, and H. K. Mao, *Phys. Rev. Lett.* **82**, 3284 (1999).
- [40] J. Badro, J.-P. Rueff, G. Vanko, G. Monaco, G. Fiquet, and F. Guyot, *Science* **305**, 383 (2004).
- [41] R. Lengsdorf, J.-P. Rueff, G. Vanko, T. Lorenz, L. H. Tjeng, and M. M. Abd-Elmeguid, *Phys. Rev. B* **75**, 180401 (2007).
- [42] A. Mattila, T. Pylkkanen, J.-P. Rueff, S. Huotari, G. Vanko, M. Hanand, M. Lehtinen, and K. Hamalainen, *J. Phys.: Condens. Matter* **19**, 386206 (2007).
- [43] G. Vanko, J.-P. Rueff, A. Mattila, Z. Nemeth, and A. Shukla, *Phys. Rev. B* **73**, 024424 (2006).
- [44] M. Croft, D. Sills, M. Greenblatt, C. Lee, S.-W. Cheong, K. V. Ramanujachary, and D. Tran, *Phys. Rev. B* **55**, 8726 (1997).
- [45] V. V. Poltavets, M. Croft, and M. Greenblatt, *Phys. Rev. B* **74**, 125103 (2006).
- [46] Z. Hu, G. Kaindl, and G. Meyer, *J. Alloys Compd.* **246**, 186 (1997).
- [47] A. Bianconi, A. Marcelli, H. Dexpert, R. Karnatak, A. Kotani, T. Jo, and J. Petiau, *Phys. Rev. B* **35**, 806 (1987).
- [48] Z. Hu, S. Bertram, and G. Kaindl, *Phys. Rev. B* **49**, 39 (1994).
- [49] Z. Hu, G. Kaindl, D. Vandr e, R. Hoppe, and G. Wortmann, *J. Alloys Compd.* **205**, 263 (1994).
- [50] Z. Hu, G. Kaindl, and B. G. M uller, *J. Alloys Compd.* **246**, 177 (1997).
- [51] D. Cao, F. Bridges, S. Bushart, E. D. Bauer, and M. B. Maple, *Phys. Rev. B* **67**, 180511(R) (2003).
- [52] J. M. Chen, Y. Y. Chin, M. Valldor, Z. Hu, J. M. Lee, S. C. Haw, N. Hiraoka, H. Ishii, C. W. Pao, K. D. Tsuei, J. F. Lee, H. J. Lin, L. Y. Jang, A. Tanaka, C. T. Chen, and L. H. Tjeng, *J. Am. Chem. Soc.* **136**, 1514 (2014).